Modeling the Nonlinear, Strain Rate Dependent Deformation of Shuttle Leading Edge Materials with Hydrostatic Stress Effects Included

Robert K. Goldberg and Kelly S. Carney

NASA Glenn Research Center
Cleveland, OH

Abstract

An analysis method based on a deformation (as opposed to damage) approach has been developed to model the strain rate dependent, nonlinear deformation of woven ceramic matrix composites, such as the Reinforced Carbon Carbon (RCC) material used on the leading edges of the Space Shuttle. In the developed model, the differences in the tension and compression deformation behaviors have also been accounted for. State variable viscoplastic equations originally developed for metals have been modified to analyze the ceramic matrix composites. To account for the tension/compression asymmetry in the material, the effective stress and effective inelastic strain definitions have been modified. The equations have also been modified to account for the fact that in an orthotropic composite the in-plane shear response is independent of the stiffness in the normal directions. The developed equations have been implemented into LS-DYNA through the use of user defined subroutines (UMATs). Several sample qualitative calculations have been conducted, which demonstrate the ability of the model to qualitatively capture the features of the deformation response present in woven ceramic matrix composites.

Introduction

In the analysis of the impact behavior of foam on the leading edge of the Space Shuttle, accurate modeling of the deformation response of the Reinforced Carbon Carbon (RCC) leading edge material, a woven ceramic matrix composite with a plain weave fabric pattern, is critical. However, this material has several characteristics in the macroscopic deformation response which make material modeling efforts challenging. The stress-strain curve for this material is nonlinear, and the deformation response changes with strain rate. Furthermore, the uniaxial tension and compression responses are different, which implies that on the macroscopic scale the hydrostatic stresses have an effect on the material response.

In ongoing work at NASA Glenn Research Center, efforts to analyze this material using LS-DYNA material model 58, MAT_LAMINATED_COMPOSITE_FABRIC, have been reasonably successful (Carney et al 2004). However, there are several features of model 58 which indicate that examining alternative methods of simulating the material response would be beneficial. First of all, in model 58 strain rate dependence of the material behavior is not explicitly accounted for within the model. However, in preliminary tests on the RCC material the data have indicated that this material may indeed have a nontrivial rate dependence. While preliminary efforts are underway to investigate adding strain rate dependence to model 58, these efforts are incomplete at this time. Furthermore, in model 58 all of the nonlinearity of the deformation response is due to damage mechanisms instead of deformation mechanisms (Matzenmiller et al 1995). Providing an alternative modeling capability in which the nonlinearity in the deformation response is assumed to be due to deformation mechanisms, allowing for a decoupling of the deformation and damage/failure response, could be more representative of the actual physical behavior. This is particularly true in this case since in the

theory on which model 58 is based (Matzenmiller et al 1995), the assumptions used to develop the damage/failure criteria applied in the equations were based on behaviors representative of polymer matrix composites. These assumptions may not necessarily be absolutely valid for the ceramic matrix composite material which is used for the Space Shuttle leading edges.

At NASA Glenn Research Center, efforts have been underway for several years to model the strain rate dependent, nonlinear deformation of polymers with the effects of hydrostatic stresses included. In these efforts, the Bodner-Partom viscoplasticity model based on the state variable approach (Bodner 2002), originally developed for metals, has been modified in order to incorporate the hydrostatic stress effects known to be present in polymers (Goldberg et al 2003). These variations include modifying the effective stress and effective inelastic strain definitions, based on an application of the Drucker-Prager yield criterion (Khan and Huang 1995), to account for the effects of the hydrostatic stresses.

In this paper, the constitutive equations with an associative flow rule described above have been applied and modified in order to model the nonlinear, strain rate dependent, deformation of plain weave woven ceramic matrix composites, including RCC, in which the differences in the tensile and compressive response are accounted for within the equations. Due to the plain weave fabric geometry of the RCC, for the purposes of this study the material is assumed to be isotropic in the normal directions, even though RCC is a composite and not a homogenous material. However, since RCC is indeed an orthotropic material on the macroscopic level, the shear response is assumed to be uncoupled from and independent of the normal response. The full theoretical development of the constitutive equations will be described in this paper, along with the procedures to be used to determine the material constants. The procedures used to implement the equations within LS-DYNA through the use of user defined subroutines will also be described. Finally, several sample calculations will be presented which will demonstrate the ability of the model to qualitatively capture the features of the deformation response of plain weave woven ceramic matrix composite materials.

Theoretical Development

To analyze the nonlinear, strain rate dependent deformation of plain weave woven ceramic matrix composites, the Bodner-Partom viscoplastic state variable model (Bodner 2002), which was originally developed to analyze the viscoplastic deformation of metals above one-half of the melting temperature and has been successfully used in such instances, has been modified. In state variable models, a single unified strain variable is defined to represent all inelastic strains (Stouffer and Dame 1996). Furthermore, in the state variable approach there is no defined yield stress. Inelastic strains are assumed to be present at all values of stress, the inelastic strains are just assumed to be very small in the "elastic" range of deformation. State variables, which evolve with stress and inelastic strain, are defined to represent the average effects of the deformation mechanisms.

An important point to note is that frequently, in state variable models, each of the state variables and material constants have a fairly explicit link to specific deformation mechanisms, such as dislocation pileups in metals (Stouffer and Dame 1996). Here, due to the complex nature of the material deformation mechanisms in woven ceramic matrix composites the linkage between the state variables and material constants to specific deformation mechanisms is not nearly as well defined. For this work, an internal stress state variable is defined to represent phenomelogically the resistance to inelastic deformation, a state variable is defined to represent the effects of hydrostatic stresses and a state variable is defined in order to scale the shear

stresses to ensure a consistent effective stress. The material constants are characterized in order to correlate with the experimentally observed deformation of the material, and are not tightly linked to specific deformation mechanisms. However, the equations developed here employ a fairly simple formulation with a minimum of material constants that are fairly simple to characterize, and capture the main features of the deformation response.

For this study, temperature and moisture effects have been neglected, as only room temperature data are currently available. All of the nonlinearity and strain rate dependence observed in the material is assumed in this work to be due to inelastic deformation, where in reality the nonlinearity is most likely due to a mixture of deformation and damage. Furthermore, as mentioned previously in reality plain weave woven ceramic matrix composites like RCC are orthotropic materials, as is typical of composites. However, due to the plain weave architecture of the fibers, the material can be assumed to be isotropic in the normal directions, with independent shear responses.

Associated Flow Equation and Evolution Equations

In order to derive the associated flow equation for the components of the inelastic strain rate tensor for plain weave woven ceramic matrix composites with hydrostatic stress effects (different responses in tension and compression) included, a procedure similar to that employed to derive the Prandtl-Reuss equations in classical plasticity is utilized (Khan and Huang 1995) (Stouffer and Dame 1996). The formulation employed in this study is based on that used by Pan and co-workers (Li and Pan 1990) (Chang and Pan 1997) and Hsu, et al (Hsu et al. 1999). First, an inelastic potential function based on the Drucker-Prager yield criterion (Khan and Huang 1995) is defined as

$$f = \sqrt{J_2^*} + \alpha \sigma_{kk} \tag{1}$$

where σ_{kk} is the sum of the normal stress components (assuming the usual rules of indicial notation (Stouffer and Dame 1996)) and is equal to three times the hydrostatic stress. The variable α is a state variable which controls the level of the hydrostatic stress effects. The term "$\alpha\sigma_{kk}$" incorporates the effects of hydrostatic stresses into the inelastic potential function. The variable J_2^* is a modified version of the second invariant of the deviatoric stress tensor. The modification is required due to the fact that for the orthotropic composites examined here the shear responses are independent of the normal terms in the stiffness matrix. Therefore, in order to ensure a consistent effective stress, the shear stresses must be multiplied by a scaling state variable β. The modified version of the deviatoric second invariant is given as follows

$$J_2^* = \frac{1}{6}\left[(\sigma_{11}-\sigma_{22})^2 + (\sigma_{22}-\sigma_{33})^2 + (\sigma_{33}-\sigma_{11})^2\right] + \beta\left[\sigma_{12}^2 + \sigma_{13}^2 + \sigma_{23}^2\right] \tag{2}$$

where σ_{ij} are the components of the stress tensor. Note that for the current work all three shear stress components are scaled by the same value of β. In actuality, each shear stress component may require a unique scaling factor. However, for the current work the model is implemented using thin shell elements, which results in the transverse shear stresses being approximate at best. Furthermore, at the current time only in-plane shear data is available to be examined. As a result, only the correct scaling of the in-plane shear stresses is considered significant for this work. The effects of possible errors in the scaling of the transverse shear stresses are assumed to

not be significant. The components of the inelastic strain rate tensor, $\dot{\varepsilon}_{ij}^I$, are assumed to be proportional to the derivative of the potential function with respect to the components of the stress tensor, σ_{ij}, as follows

$$\dot{\varepsilon}_{ij}^I = \dot{\lambda}\frac{\partial f}{\partial \sigma_{ij}}$$

(3)

where $\dot{\lambda}$ is a scalar rate variable. By taking the specified derivative of the potential function, the result becomes

$$\frac{\partial f}{\partial \sigma_{ij}} = \frac{S_{ij}^*}{2\sqrt{J_2}} + \alpha\delta_{ij}$$

(4)

where δ_{ij} is the Kronecker delta and S_{ij}^* are the modified components of the deviatoric stress tensor. For the normal stress components, S_{ij}^* is equal to S_{ij}, the components of the deviatoric stress tensor. However, to maintain consistency, for the shear stress components the terms are scaled as follows

$$S_{ij}^* = \left(\sqrt{\beta}\right)\sigma_{ij}$$

(5)

where β is the shear scaling state variable discussed earlier.

The next step in defining the flow rule is to define the effective stress and the effective inelastic strain rate. The effective stress, σ_e, is defined as follows

$$\sigma_e = \sqrt{3}f = \sqrt{3J_2^*} + \sqrt{3}\alpha\sigma_{kk}\,.$$

(6)

To determine the value of the scalar $\dot{\lambda}$ in terms of the effective inelastic strain rate, $\dot{\varepsilon}_e^I$, the principal of the equivalence of the inelastic work rate is employed. With the aid of Equations 3 and 4, the inelastic work rate, $\dot{W}^I$, can be expressed by the following

$$\dot{W}^I = \sigma_{ij}\dot{\varepsilon}_{ij}^I = \sigma_{ij}\left(\frac{S_{ij}^*}{2\sqrt{J_2}} + \alpha\delta_{ij}\right)\dot{\lambda} = \sigma_e\dot{\varepsilon}_e^I\,.$$

(7)

After applying the effective stress definition given in Equation 6 and simplifying, it can be shown that

$$\dot{\lambda} = \sqrt{3}\dot{\varepsilon}_e^I$$

(8)

By substituting Equation 8 and Equation 4 into Equation 3, a definition for the components of the inelastic strain rate tensor can be given as

$$\dot{\varepsilon}_{ij}^{I} = \sqrt{3}\dot{\varepsilon}_{e}^{I}\left(\frac{S_{ij}^{*}}{2\sqrt{J_{2}}} + \alpha\delta_{ij}\right). \tag{9}$$

By utilizing Equation 7, it can be shown that the effective inelastic strain rate can be defined as

$$\dot{\varepsilon}_{e}^{I} = \dot{e}_{e}^{I} = \sqrt{\frac{2}{3}\left[\left(\dot{e}_{11}^{I}\right) + \left(\dot{e}_{22}^{I}\right)^{2} + \left(\dot{e}_{33}^{I}\right)^{2}\right] + \frac{4}{3}\kappa^{2}\left[\left(\dot{e}_{12}^{I}\right) + \left(\dot{e}_{13}^{I}\right)^{2} + \left(\dot{e}_{23}^{I}\right)^{2}\right]}$$

$$\dot{e}_{ij}^{I} = \dot{\varepsilon}_{ij}^{I} - \dot{\varepsilon}_{m}^{I}\delta_{ij} \tag{10}$$

where $\dot{e}_{e}^{I}$ is the effective deviatoric inelastic strain rate and $\dot{\varepsilon}_{m}^{I}$ is the mean inelastic strain rate. The inelastic shear strain rates need to be scaled by a constant scale factor κ due to the fact that for an orthotropic material the shear terms in the stiffness response are independent of the normal terms. When κ equals one, which would happen for isotropic materials, the inelastic strain rate definition given here matches the effective inelastic strain rate definition given by Pan and co-workers (Li and Pan 1990) (Chang and Pan 1997).

By following a similar format to the Bodner-Partom model (Bodner 2002) (Stouffer and Dame 1996), the following definition is specified

$$\frac{\sqrt{3}}{2}\dot{\varepsilon}_{e}^{I} = D_{o}\exp\left[-\frac{1}{2}\left(\frac{Z}{\sigma_{e}}\right)^{2n}\right] \tag{11}$$

where D_{o} and n are material constants. D_{o} represents the maximum inelastic strain rate, and n controls the rate dependence of the material. Z is an isotropic state variable which represents the resistance to inelastic deformation (internal stress). By substituting Equation 11 into Equation 9, the final form of the flow equation is determined to be

$$\dot{\varepsilon}_{ij}^{I} = 2D_{o}\exp\left[-\frac{1}{2}\left(\frac{Z}{\sigma_{e}}\right)^{2n}\right]\left(\frac{S_{ij}}{2\sqrt{J_{2}}} + \alpha\delta_{ij}\right). \tag{12}$$

Note that the elastic components of the strain rate must be added to the inelastic strain rate to obtain the total strain rate.

The rate of evolution of the internal stress state variable Z, the hydrostatic stress effect state variable α and the shear scaling factor state variable β are defined by the equations

$$\dot{Z} = q(Z_{1} - Z)\dot{e}_{e}^{I} \tag{13}$$

$$\dot{\alpha} = q(\alpha_{1} - \alpha)\dot{e}_{e}^{I} \tag{14}$$

$$\dot{\beta} = q(\beta_{1} - \beta)\dot{e}_{e}^{I} \tag{15}$$

where q is a material constant representing the "hardening" rate, and Z_{1}, α_{1} and β_{1} are material constants representing the maximum values of Z, α and β respectively. The initial values of Z, α

and β are defined by the material constants Z_o, α_o and β_o. The term $\dot{e}_e^I$ in Equations 13, 14 and 15 represents the effective deviatoric inelastic strain rate, which was defined in Equation 10. An important point to note is that in the original Bodner model (Bodner 2002), the inelastic work rate was used instead of the effective inelastic strain rate in the evolution equation for the internal stress state variable. However, for this work the inelastic strain rate was deemed easier to work with from both computational and characterization points of view, particularly in the incorporation of hydrostatic stress effects. Furthermore, the effective inelastic strain rate has been used in other state variable constitutive models (Stouffer and Dame 1996). Since hydrostatic stress effects were not considered in the original Bodner model (Bodner 2002), the evolution equation for α is new to this work. Furthermore, since these equations were originally developed for homogenous isotropic materials and not composites, the evolution equation for β is also new to this work. The state variables α and β are assumed to evolve in the same manner as the state variable Z. By using this assumption the value of q used in Equations 14 and 15 can be shown to be the same as the value of q used in Equation 13.

Determination of Material Constants

The material constants that need to be determined include D_0, n, Z_o, Z_1, α_o, α_1, β_o, β_1, κ and q. These values, along with the elastic modulus, shear moduli and Poisson's ratio are the input parameters required for the model. The procedure to be used is summarized here. More details on the procedure as it was used for isotropic polymers can be found in Goldberg, et al. (Goldberg et al 2003). The constants are determined using tensile and compressive stress-strain curves obtained from a set of constant strain rate tests, along with a shear stress-shear strain curve obtained for at least one strain rate. Each tension and compression test is conducted at a different total strain rate.

The first step in the process is to obtain the values of α_1 and α_o. To accomplish this task, Equation 6 is used in combination with stress-strain data from constant strain rate uniaxial tension and compression tests. The values of these constants are assumed to be rate independent, so the results from only one strain rate need to be used to find the needed parameters. In practical application of the methodology, the uniaxial tension and compression tests used do not have to be at the exact same effective strain rate. As long as the effective strain rates from the two tests are approximately equal, the values obtained have been found to be valid, particularly if quasi-static strain rates are examined. Two stress values from the tensile and compressive stress-strain curves are required in order to find these two constants. First of all, the "saturation stress", the stress level at which the stress-strain curve flattens out and becomes horizontal, is required. At this stress level, the inelastic strain rate is assumed to be equal to the total applied strain rate. If the actual stress-strain curve terminates before the saturation stress is reached (as often happens in compression), the curve must be extrapolated to obtain an approximate value of the saturation stress. Secondly, the stress level at which the tension and compression curves becomes nonlinear (the "yield" stress), is required. One important point needs to be considered when determining the stress level designating the onset of nonlinearity. Frequently, in woven ceramic matrix composites, the tensile stiffness across nearly the entire stress-strain curve tends to be significantly softer than the compressive stiffness, most likely due to the fact that in tension significant matrix microcracks develop almost immediately upon loading, which weakens the material. As a result, in cases where this phenomena occurs the initial portion of the compression curve is assumed to represent the "elastic" regime of the composite material, and in tension the onset of nonlinearity in the stress-strain curve is assumed to occur at a very small, almost negligible stress value.

Given these definitions, Equation 6 can now be used to determine the values of α_1 and α_o. The primary assumption used at this point (and assumed implicitly in Equation 6) is that the effective stress at saturation under uniaxial tensile loading at a particular strain rate is equal to the effective stress at saturation under compression loading at the same equivalent strain rate. Likewise, the effective stress at the point the stress-strain curve becomes nonlinear under tensile loading is equal to the effective stress at the point the stress-strain curve becomes nonlinear under compression loading. Therefore, assuming the value of α at saturation is equal to α_1, and the value of α at the point the stress-strain curve becomes nonlinear is equal to α_o, the following equations are obtained for the case of having data from uniaxial tension and compression tests

$$\sigma_{st}\left(1+\sqrt{3}\alpha_1\right)=\sigma_{sc}\left(1-\sqrt{3}\alpha_1\right) \tag{16}$$

$$\sigma_{nlt}\left(1+\sqrt{3}\alpha_o\right)=\sigma_{nlc}\left(1-\sqrt{3}\alpha_o\right) \tag{17}$$

where σ_{st} and σ_{sc} are the tensile and compressive stresses at saturation, respectively, and σ_{nlt} and σ_{nlc} are the tensile and compressive stresses at the point where the respective stress-strain curves become nonlinear. Therefore, by substituting the tensile and compressive stresses at saturation into this equation, followed by the tensile and compressive stresses at the point where the respective stress-strain curves become nonlinear, the required constants can be determined. At this point, by applying Equation 6 for the tensile and shear curves, using the appropriate "saturation" and "yield" stresses in tension and shear, the values of β_o and β_1 can be determined from the following equations

$$\sigma_{st}\left(1+\sqrt{3}\alpha_1\right)=\sqrt{3\beta_1}\,\tau_s \tag{18}$$

$$\sigma_{nlt}\left(1+\sqrt{3}\alpha_o\right)=\sqrt{3\beta_o}\,\tau_{nl} \tag{19}$$

where σ_{st} and τ_s are the tensile and shear stresses at saturation, respectively, and σ_{nlt} and τ_{nl} are the tensile and shear stresses at the point where the respective stress-strain curves become nonlinear.

The values of D_0, n, and Z_1 are characterized as follows. The value of D_0 is currently assumed to be equal to a value of 10^4 times the maximum applied strain rate, which correlates with the maximum inelastic strain rate. To determine the values of n and Z_1, first Equation 12 is simplified to the case of uniaxial tensile loading, leading to the following expression

$$\dot{\varepsilon}^I = 2D_0 \exp\left[-\frac{1}{2}\left(\frac{Z}{(1+\sqrt{3}\alpha)\sigma}\right)^{2n}\right]\left(\frac{\sigma}{\sqrt{3}|\sigma|}+\alpha\right) \tag{20}$$

where $\dot{\varepsilon}^I$ is the uniaxial tensile inelastic strain rate in a constant strain rate tensile test, σ is the uniaxial tensile stress, and the remainder of the terms are as defined earlier. The case of uniaxial tensile loading is used to determine these constants since for woven ceramic matrix composites the tensile stress-strain curves obtained experimentally are more likely to display a defined "saturation" stress than the compression curves, which as shown below is crucial for determining the material constants. Furthermore, Equation 20 can be rearranged as follows

$$-2\ln\left(\frac{\dot{\varepsilon}^{I}}{2D_0\left(\frac{1}{\sqrt{3}}+\alpha\right)}\right) = \left(\frac{Z}{(1+\sqrt{3}\alpha)\sigma}\right)^{2n} \quad . \tag{21}$$

The required constants are determined from a set of tensile stress-strain curves obtained from constant strain rate tests. Each curve in this set is obtained at a different constant strain rate. Data pairs of the total strain rate (equal to the inelastic strain rate at saturation) and saturation stress values from each curve are taken. For each strain rate, the data values are substituted into Equation 21, after the natural logarithm of both sides of the equation is taken, and represent a point on a master curve. The number of points in the master curve equals the number of strain rates at which the tensile tests were conducted. A least squares regression analysis is then performed on the master curve. As can be shown from Equation 21, the slope of the best-fit line is equal to -2n. The intercept of the best-fit line is equal to 2n(ln (Z_1)).

To determine the value of Z_o, Equation 21 can be used again. In this case, the value of the tensile stress where the stress-strain curve becomes nonlinear for a particular constant strain rate tensile test is used, as well as the value of the approximate inelastic strain rate when the stress-strain curve becomes nonlinear. The point where the stress-strain curve becomes nonlinear is defined as the approximate point where the curve appreciably deviates from a linear extrapolation of the initial data. The strain rate used in the constant strain rate test divided by 100 was found by trial and error to approximate the inelastic strain rate at this point reasonably well. Using this data, Equation 21 is solved for Z, which is assumed to be equal to the value of Z_o. Compression data can also be used, particularly for the case when the tensile stress at which the stress-strain curve becomes nonlinear is approximated due to the differences in the initial tension and compression responses as discussed above. In this case, Equations 20 and 21 need to be reformulated based on Equation 12 given that compressive stresses are being considered as opposed to tensile stresses. Another point to note is that using the data from the lowest strain rate test available has been found to give adequate values of Z_o. However, the calculations can be made using data from all the available strain rates, and an average taken if required to obtain the value of the constant.

To determine the value for q for Equations 13, 14 and 15, first Equation 13 is integrated for the case of pure tensile loading (again since for woven ceramic matrix composites the tensile curves are more likely to display a distinct saturation stress), resulting in the following relation

$$Z = Z_1 - (Z_1 - Z_o)\exp\left(-q\varepsilon_e^{I}\right) \tag{22}$$

where ε_e^{I} is the effective inelastic strain, computed using Equation 10. At saturation, the value of the internal stress Z is assumed to approach Z_1, resulting in the exponential term approaching zero. Assuming that saturation occurs when the following condition is satisfied

$$\exp\left(\frac{-q\varepsilon_s^{I}}{1+\sqrt{3}\alpha}\right) = 0.01 \tag{23}$$

the equation is solved for q, where ε_s^I is the inelastic tensile strain at saturation. Also, in Equation 23 the effective inelastic strain at saturation is simplified to the case of uniaxial tensile loading through the use of Equations 9 and 10. If the inelastic strain at saturation is found to vary with strain rate, the parameter q is computed at each strain rate and regression techniques are utilized to determine an expression for the variation of q. If Equations 14 and 15 are integrated, an expression similar to Equation 23 is obtained. At saturation, the values of α and β are assumed to approach α_1 and β_1, and equations identical to Equation 23 are obtained, which would lead to the same value for q. Therefore, identical values of q are used in Equations 13, 14 and 15.

To find the value of κ, Equation 10 is used along with results from a uniaxial tensile test and a pure shear test. Specifically, the effective inelastic strain at saturation for a tensile test at a particular total strain rate (usually the lowest) is set equal to the effective inelastic strain at saturation from a pure shear test at the same approximate total strain rate, resulting in the following expression which can be solved for κ

$$\frac{\varepsilon_s^I}{1+\sqrt{3}\alpha} = \frac{\kappa\gamma_s^I}{\sqrt{3}} \tag{24}$$

where ε_s^I is once again the inelastic tensile strain at saturation and γ_s^I is the inelastic engineering shear strain at saturation.

Finite Element Implementation

The constitutive equations described above have been implemented into LS-DYNA through the use of the user defined subroutine (UMAT) option. The routines are designed to work with shell elements, therefore the equations are specialized for the case of plane stress in the normal directions. A composite is a thin structure, which justifies the use of shell elements. The use of shell elements allows greater flexibility in terms of defining a laminate of many composite plies, and in specifying the angle of orientation of the material. Furthermore, the use of shell elements provides greater flexibility and computational efficiency in terms of analyzing a complex structure. All of the material constants are entered into the input deck. The history variables for the finite element analysis are defined to include the deviatoric stresses, the hydrostatic stress, the values of the state variables and the inelastic strain rate tensor. To integrate the constitutive equations, both a standard Euler integrator (Kreyszig 1992) and a fourth order Runge-Kutta integrator (Kreyszig 1992) have been implemented within separate UMAT routines. The Euler routine is very simple to define and implement. However, in order to ensure accurate results, each time step must be broken up into ten mini-steps within the UMAT routine. The Runge-Kutta routine, while somewhat more complex to implement, does not require the time step division within the routine. Studies are still being carried out as to which integrator yields the most accurate answers with the greatest computational efficiency.

In the UMAT routine, the material constants and the current values of the history variables are read into the routine. The values of the elastic stiffness tensor are computed based on the elastic modulus and Poisson's ratio. Within the integration routines, for each integration step the effective stress is computed employing the current stress values and the current value of the state variable α using Equation 6. Next, the terms in the inelastic strain rate tensor are determined using Equation 12. The effective inelastic strain rate is determined using Equation 10, and then the state variable rates are determined using Equations 13, 14 and 15. The appropriate

integration formula and time step increment is then used to compute updated values of the inelastic strain increments and the state variables. From the given total strain increments and the computed inelastic strain increments, along with the elastic constants, the values which are computed include the strain increments for the current step in the integration process, the stress increments and revised total stresses. In this process, the out of plane normal strain increments are calculated in a manner such that the plane stress condition is enforced, and the out of plane normal stress is set equal to zero. As is common for shell elements, a correction factor of 0.833 is used in computing the transverse shear stresses. Revised values of the deviatoric and hydrostatic stresses determined from the computed stresses, and the integration process is continued as required. Finally, the history variables are written out, and the routine returns.

Sample Calculations

To demonstrate the ability of the model described above to qualitatively capture the features of the deformation response of woven ceramic matrix composites such as RCC, several sample analyses have been carried out using the current model. The tension, compression and shear stress-strain curves for a representative woven ceramic matrix composite with a plain weave fiber architecture were determined and are shown qualitatively in Figure 1. Specific numerical values for the stress-strain curve, the material constants that were utilized and comparisons to actual test data cannot be presented at this time due to formal NASA restrictions on the use and discussion of actual data on the RCC material. However, as can be seen from the presented stress-strain curves, the nonlinearity of the deformation response most likely present in actual experimental data is captured well. Furthermore, the presented computations demonstrate the ability of the constitutive equations to capture qualitatively the significant differences in the tension and compression responses using a single set of material constants. In Figure 2, tensile stress-strain curves at two different strain rates are generated. As can be seen in the figure, the model is able qualitatively to capture strain rate dependencies in the material response, which again is a factor in the actual deformation response of these materials. Future efforts will involve further exercising the model and comparing the computed results to publicly available test data.

Conclusions

The Bodner-Partom viscoplastic state variable model (Bodner 2002) has been modified in order to analyze the strain rate dependent, nonlinear deformation of woven ceramic matrix composites such as the Reinforced Carbon Carbon found in Space Shuttle leading edges. The differences in the tensile and compressive deformation responses have been accounted for through the modification of the effective stress and effective inelastic strain definitions given in the original equations. The procedures used to compute the shear response have also been modified to account for the fact that in an orthotropic composite the shear response is independent of the normal response. The material constants can be obtained based on tension, compression and shear tests. The constitutive equations have been implemented within LS-DYNA through the use of the user defined subroutine (UMAT) option. Sample calculations have been conducted which demonstrate the ability of the model to qualitatively capture the nonlinearity, strain rate dependence and tension/compression asymmetry observed in the deformation response of woven ceramic matrix composites such as Reinforced Carbon Carbon.

References

Bodner, S.R., *Unified Plasticity for Engineering Applications*, Kluwer Academic/Plenum Publishers, New York (2002).

Carney, K.S.; Melis, M.E.; Fasanella, E.L.; Lyle, K.H.; and Gabrys, J., "Material Modeling of Space Shuttle Leading Edge and External Tank Materials For Use in the Columbia Accident Investigation", 8th International LS-DYNA Users Conference, May 2-4, 2004, Dearborn, MI (2004).

Chang, W.J. and Pan, J., "Effects of Yield Surface Shape and Round-Off Vertex on Crack-Tip Fields for Pressure-Sensitive Materials", Vol. 34, p. 3291-3320, International Journal of Solids and Structures, (1997).

Goldberg, R.K.; Roberts, G.D.; and Gilat, A., "Implementation of an Associative Flow Rule Including Hydrostatic Stress Effects Into the High Strain Rate Deformation Analysis of Polymer Matrix Composites", NASA/TM-2003-212382 (2003).

Hsu, S.-Y., Vogler, T.J., and Kyriakides, S. (1999). "Inelastic behavior of an AS4/PEEK composite under combined transverse compression and shear. Part II: modeling", Vol. 15, p.807-836, International Journal of Plasticity, (1999).

Khan, A.S. and Huang, S. *Continuum Theory of Plasticity*, John Wiley and Sons, New York (1995).

Kreyszig, E., *Advanced Engineering Mathematics, 7th Edition*, John Wiley and Sons, New York (1992).

Li, F.Z and Pan, J., "Plane-Stress Crack-Tip Fields for Pressure-Sensitive Dilatant Materials", Vol. 57, p. 40-49, Journal of Applied Mechanics (1990).

Matzenmiller, A.; Lubliner, J.; and Taylor, R.L., "A constitutive model for anisotropic damage in fiber-composites", Vol. 20, p. 125-152, Mechanics of Materials (1995).

Stouffer, D.C. and Dame, L.T., *Inelastic Deformation of Metals. Models, Mechanical Properties and Metallurgy*, John Wiley and Sons, New York (1996).
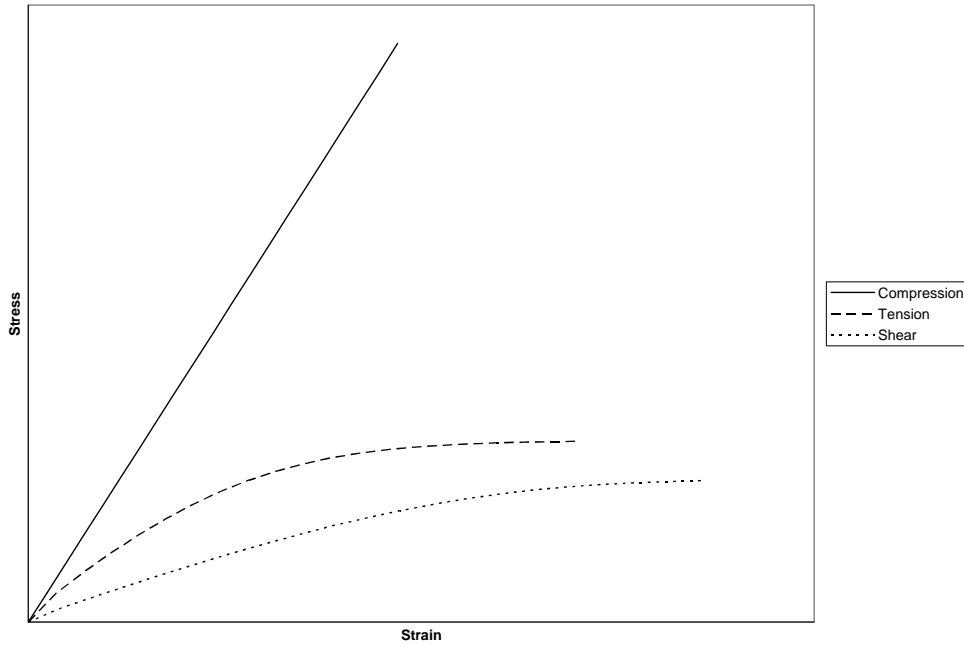
Figure 1: Computed tension, compression and shear deformation of a representative woven ceramic matrix composite material.
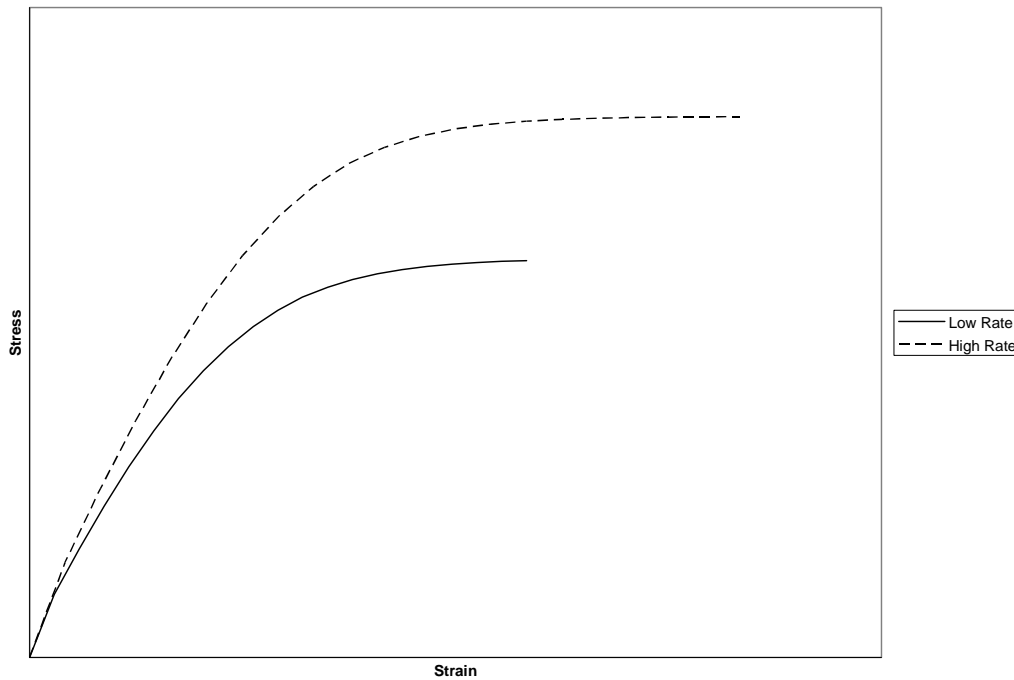

Figure 2: Effect of strain rate on the tensile deformation of a representative woven ceramic matrix composite material.